Quantitative Stress-Redistribution Thallium-201 SPECT Using Prone Imaging: Methodologic Development and Validation

Hosen Kiat, Kenneth F. Van Train, John D. Friedman, Guido Germano, Gerard Silagan, Fan Ping Wang, Jamshid Maddahi, Florence Prigent, and Daniel S. Berman

Departments of Medicine (Division of Cardiology) and Nuclear Medicine, Cedars-Sinai Medical Center, University of California School of Medicine, Los Angeles, California

Prone ^{201}Tl myocardial perfusion SPECT has been shown to improve left ventricular inferior wall counts compared to supine imaging, thus minimizing diaphragmatic attenuation. Prone SPECT quantitative normal limits were developed and prospectively applied to 36 patients who had coronary angiography. The prone imaging table used had a cut-out under cardiac area which increased the average myocardial counts by 10.7% compared to prone SPECT through the standard table. Overall specificity and sensitivity were 80% and 93%, respectively. For the right, left circumflex and left anterior descending coronary arteries, the specificities were 94%, 71%, and 94%; and sensitivities were 88%, 89% and 78%, respectively. The normalcy rate in 55 normal patients was 89%. Incidence and the severity of patient motion in 200 prone SPECT studies were compared to 200 supine SPECT studies. Mild and severe motion occurred in 12% and 4% of the supine studies and in only 3.5% and none of the prone studies, respectively. When compared to supine SPECT, prone SPECT had higher ($p < 0.01$) regional counts/pixel in the inferior wall and septum, but required an average increase of 2.9 ± 1.0 cm in camera to chest wall distance and resulted in a reduction of total myocardial counts. Prone SPECT provides an alternative approach for patients who cannot tolerate supine imaging. It should be considered when inferior wall defects on supine imaging pose a diagnostic dilemma and when motion on supine imaging necessitates repeat acquisition.

1992; 33:1509–1515

Traditionally, image acquisition of ^{201}Tl single-photon emission computerized tomography (SPECT) has been performed with the patient in the supine position. Supine tomographic images however, frequently demonstrate relative reduction of ^{201}Tl activity in the left ventricular inferior wall, presumably due to increased attenuation of photons from that region. Such attenuation of myocardial tracer activity occasionally results in false-positive findings for the diagnosis of right coronary artery disease. Recently, Esquerre et al. (*1*) demonstrated that compared to ^{201}Tl supine SPECT, tomographic images acquired in the prone position have significantly higher ^{201}Tl counts in the inferior wall, thus largely negating the problem of inferior wall attenuation. Furthermore, by visual interpretation, ^{201}Tl SPECT acquired in the prone position has been shown to improve the overall specificity for detection of patients with coronary artery disease as well as right coronary artery disease specificity (*2*). The purpose of this work is to develop ^{201}Tl prone SPECT quantitative normal limits, to evaluate the diagnostic efficacy of ^{201}Tl SPECT acquired in the prone position and to compare the frequency of patient motion during SPECT acquisition.

Received Dec. 3, 1991; revision accepted Mar. 10, 1992.

For reprints contact: Daniel S. Berman, MD, Cedars-Sinai Medical Center, 8700 Beverly Blvd., Los Angeles, CA 90048.

SUBJECTS AND METHODS

Entry Criteria

The study employed prospective male patients who had ^{201}Tl prone SPECT performed on the cut-out table. These were consecutive patients who either had cardiac catheterization performed within 3 mo of ^{201}Tl testing or who had a low (<5%) likelihood of coronary artery disease based on age, sex, symptoms and results of stress electrocardiography (*3–5*). Patients with prior coronary bypass surgery or balloon angioplasty, and those who achieved <85% of maximal predicted heart rate without ischemic exercise end-point (chest pain or ST-segment depression) were excluded.

We have not included a female population since we feel, that due to the presence of breast tissue, prone imaging is not as suitable for the female population, from the point of view of both patient comfort and the potential accentuation of artifactual breast attenuation defects.

Patient Population

Diagnostic efficacy of prone SPECT was assessed in 111 males with a mean age of 59 ± 12 yr. Of the 36 patients who had cardiac catheterization, 30 had coronary artery disease (defined as ≥50% stenosis in ≥1 major coronary vessels), and 6 had normal coronary arteriograms. The data of one patient with normal coronary arteriogram could not be retrieved from the computer tape for quantitative analysis, but the images were included for visual analysis. Twelve of the 36 patients had historically documented

prior myocardial infarction. There were a total of 75 patients with a low likelihood of coronary artery disease. The data from the first twenty were used to develop quantitative prone SPECT normal limits.

To assess the potential difference of camera-to-chest wall distance as a result of imaging position, camera-to-chest wall distance for both prone and supine SPECT was measured in four patients (weight: 55–86 kg).

In addition, the frequency of patient motion was evaluated in 200 stress and redistribution ^{201}Tl SPECT studies from 100 consecutive patients undergoing prone ^{201}Tl study and was compared to another 100 consecutive patients undergoing supine ^{201}Tl SPECT. The demographics, symptoms, exercise physiology and the results of ^{201}Tl testing between the supine and prone study groups were compared in Table 1.

Exercise and Imaging Protocol

Symptom-linked treadmill was performed using the standard Bruce protocol, and 3–4 mCi of ^{201}Tl were injected at peak exercise. All patients were imaged using a rotating gamma camera (Siemens Orbiter). Prone SPECT employed a prototype imaging table with a cut-out under the cardiac area developed by Siemens Gammasonics, Inc. (Fig. 1). The table is of standard width (17 inches) and has a region of 12 × 16 in. under the cardiac area in the left mid-chest in which the structure of the table was removed and covered only by fabric. The table is supported by a steel bar wrapping around the right side, precluding 360° imaging. The SPECT acquisition and processing protocols were as previously described for ^{201}Tl SPECT (*6,7*). Specifically, for SPECT acquisition by both prone and supine imaging, the patient was centered in the field of view and the 180° circular imaging arc was selected for each patient so as to minimize the camera to chest wall distance.

Development of Quantitative Polar Map and Normal Limits

The method for ^{201}Tl SPECT quantitative analysis, including generation of polar map and normal limits, was based on the previously optimized and validated Cedars-Sinai Medical Center ^{201}Tl SPECT quantitative analysis for supine imaging (*6,7*). In short, maximum counts circumferential profiles were generated from the short- and vertical long-axis tomograms and normalized to 100. All count profiles were then mapped onto a two-dimensional polar map representing the entire left ventricular myocardium. As with our supine ^{201}Tl quantitative SPECT approach, normal limits were derived from the lowest observed values of all profiles from the 20 normal patients. The quantitative stress perfusion polar map was divided into three coronary territories. For each territory in patients with no prior myocardial infarction, abnormality was defined according to our previous work with supine ^{201}Tl SPECT (*6,7*) as a defect of ≥12% for the left anterior descending (LAD) or left circumflex (LCX) coronary arteries, respectively, or ≥8% for the right coronary artery (RCA) territory. For patients with prior myocardial infarction, the thresholds for abnormality in the individual vascular territories were modified based on previous work from our group, which considers the contiguity of a stress defect not in the vascular territory of an infarcted zone with the defects within the infarcted vascular territory (*8*). The thresholds for abnormality for defects not within an infarcted zone but contiguous with a defect in the infarcted zone were set as 12% for the LAD, 20% for the RCA and 40% for the LCX territories. For perfusion defects not contiguous with defects in the zone of prior myocardial infarction, the standard criteria were employed.

A study was considered abnormal if ≥1 vascular territories was called abnormal.

TABLE 1
Comparison of Demographics, Clinical, Exercise Physiology and ^{201}Tl Data Between Patients Undergoing Prone and Supine Stress Redistribution ^{201}Tl SPECT

	Prone	Supine	p
Total patients	100	100	
Male	85%	62%	0.0002
Age	62.4 ± 9.7	63.9 ± 11.7	ns
Weight (lbs)	173.5 ± 30.5	167.6 ± 36.2	ns
Female breast			
Bra size	36 ± 2.1	37.1 ± 3.0	ns
Cup size of ≥ C	64%	47%	ns
EX duration	7.7 ± 2.9	6.5 ± 3.0	0.008
Peak EX heart rate	143 ± 22.4	138.5 ± 22.8	ns
Peak EX BP	184.1 ± 25.9	180.6 ± 33.2	ns
EX angina	11%	15%	ns
Ischemic EX ECG	40%	31%	ns
Abnormal ^{201}Tl	55%	68%	ns

EX = exercise and BP = systolic blood pressure.

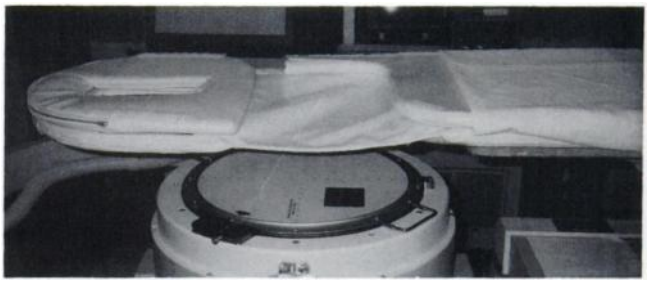

FIGURE 1. The specially designed prone imaging table demonstrating a cut-out under the cardiac area.

Assessment of Myocardial ^{201}Tl Count Statistics and Camera-to-Chest Wall Distance

For comparison of myocardial counts between supine and prone imaging, 24 patients with a low likelihood of coronary artery disease underwent SPECT acquisition in both supine and prone position. For the first 14 patients in this study (Group 1), prone imaging was followed immediately by supine imaging. For the last 10 patients (Group 2), the imaging sequence was reversed with supine SPECT preceding prone SPECT. For each stress polar map, the counts in each of the five myocardial regions (anterior, septal, inferior, lateral walls and apex), previously defined for the polar map generation (*6,7*), were summed and divided by the number of pixels in the region to give the mean counts/pixel for each region. The total myocardial counts from all low likelihood patients (Groups 1 and 2) were measured by drawing a region of interest encompassing the entire myocardial tomograms.

The minimal distance between the center of the camera detector and a marked point on the mid-chest of four patients undergoing supine and prone SPECT was measured over 10 projections 15° apart, from the 45° RAO to the left lateral positions.

Visual Interpretation

Image display methods for visual interpretation and the criteria for perfusion defect abnormality and reversibility were as previously described (*9,10*). For each study, the tomograms were divided into 20 segments, and each segment was scored by a blinded expert using a four-point system. The assignment of coronary territories to the 20 myocardial SPECT segments was based on our previous work on SPECT angiographic correlations (*11,12*).

Assessment of Patient Motion During SPECT Acquisition

For detection of patient motion (*13,14*), immediately following each tomographic acquisition, the raw projection data in a cine format were reviewed by a technologist blinded to the patients' clinical and exercise data. The cine images are then scored for patient motion using a three-point scoring system (0 = no motion, 1 = mild motion, 2 = severe motion). This quality control procedure was routinely performed for all SPECT studies.

Cardiac Catheterization

Coronary angiography and biplane left ventriculography were performed within 60 days of the scintigraphic study. No patient had a coronary event or significant worsening of cardiac symptoms in the interval between the ^{201}Tl study and coronary angiography. The angiographic data were interpreted by two experienced observers who were unaware of the ^{201}Tl scintigraphic results. In patients with prior myocardial infarction, arteries to territories with infarction were defined on the basis of location of Q-waves on ECG and/or nonreversible ^{201}Tl defects.

Cardiac Phantom Studies

Cardiac phantom studies that simulated patient imaging conditions were used to determine the count attenuation caused by prone imaging performed using a standard table (without a cut-out) versus the modified (cut-out) table. The phantom used was a modification of a commercially available phantom (Data Spectrum) consisting of an elliptical bath and cardiac, lung and spine inserts. The cardiac insert contained a uniform concentration of 2 μCi/ml of ^{201}Tl in the "myocardium" (without defects) and the "myocardium"-to-background ratio was 2:1. Prone SPECT acquisition was performed using the standard table, and was followed immediately by a second acquisition using the modified table. The average counts from a region of interest over the "myocardium" in multiple, matched raw data projection frames were used to compare the attenuation effects produced by the two tables.

Tomographic images of the phantom study were processed and are displayed in the same manner as that used for clinical studies (*9,10*). The images were inspected by three experts (HK, DSB, KVT) for presence of imaging artifacts.

Statistical Analysis

Normalcy rate was defined as the number of patients with a low likelihood of disease with normal scintigraphic patterns divided by the total number of patients with a low likelihood of disease. The terms sensitivity and specificity were applied only to the catheterized patients. The mean differences for continuous variables were compared using the Student t-test. All continuous measures were summarized as the mean ± sd. McNemar's test was used to assess the significance of the differences between sensitivities and specificities. Probability (p) values of <0.05 were considered significant. Comparisons of proportions were made using a chi-square statistic or, when appropriate, using Fisher's exact test. All computations were made using the SAS or BMDP statistical software (*15,16*).

RESULTS

Myocardial Counts and Camera-to-Chest Wall Distance

Table 2 demonstrates the mean myocardial count distribution for supine and prone imaging (using the modified table). Results from both Group 1 (prone followed by supine SPECT) and Group 2 (supine followed by prone SPECT) showed significantly higher counts in the inferior wall and septum by prone SPECT. Furthermore, for each imaging mode, both groups exhibited similar regional myocardial counts distribution.

Comparison of the total myocardial counts of the prone (with the modified table) and supine images from the low likelihood patients demonstrated reduced counts activity by prone SPECT ($1.45 \times 10^6 \pm 2.9 \times 10^5$ versus $1.54 \times 10^6 \pm 4.02 \times 10^5$, $p = 0.02$). The measurement of camera detector-to-chest wall distance demonstrated that when compared to supine acquisition prone SPECT necessitated increased camera to chest wall distance for all imaging angles over the 180° arc, by an average of 2.9 ± 1.0 cm.

TABLE 2
Comparative Regional Myocardial Counts Statistics Between Supine and Prone ^{201}Tl SPECT

Myocardial region	Group 1 (n = 14)			Group 2 (n = 10)			Total (n = 24)		
	Supine	Prone	p	Supine	Prone	p	Supine	Prone	p
Anterior	88 ± 3	87 ± 3	0.2	87 ± 3	86 ± 4	0.7	88 ± 3	87 ± 3	0.1
Septum	82 ± 5	88 ± 6	0.05	78 ± 5	86 ± 3	0.002	81 ± 6	87 ± 4	0.0001
Inferior	76 ± 5	84 ± 5	0.01	72 ± 6	84 ± 4	0.0001	75 ± 7	84 ± 4	0.001
Lateral	90 ± 3	90 ± 3	0.9	90 ± 3	93 ± 2	0.02	90 ± 3	91 ± 3	0.2
Apex	92 ± 3	94 ± 5	0.1	91 ± 3	92 ± 3	0.4	92 ± 3	93 ± 3	0.1

Group 1: Supine images were acquired immediately after prone SPECT.
Group 2: Prone imaging was performed after supine SPECT.

The mean distance was 16.3 ± 2.9 cm for prone while it was only 13.5 ± 4.1 cm for supine acquisition ($p < 0.001$).

Overall Sensitivity, Specificity and Normalcy Rates (Table 3)

By quantitative analysis, prone SPECT resulted in high overall sensitivity (93%) and specificity (80%) for detecting coronary disease in catheterized patients, as well as high normalcy rates (89%) in patients with a low likelihood of coronary artery disease. Visual analysis results were similar.

Figure 2 shows an example of ^{201}Tl prone and supine SPECT images acquired from a 63-yr-old asymptomatic male in our study population with a low pre-^{201}Tl likelihood for coronary artery disease. This patient represents an extreme example highlighting that diaphragmatic attenuation can produce a profound defect in the inferior wall not observed by prone imaging.

Individual Vessel Sensitivity and Specificity

Table 4 shows the results of individual vessel sensitivity and specificity. Of note, the RCA specificity was 94% by quantitative analysis and 89% by visual analysis. Individual vessel sensitivities were further analyzed separately for vessels supplying myocardial territories previously not involved with myocardial infarction (Table 5). With quantitative analysis, the sensitivity for detection of right coronary artery disease in territories without prior myocardial infarction remained high (91%).

Results of Cardiac Phantom Studies

For prone SPECT using the standard versus the modified table, comparison of average myocardial counts in multiple matched projection image pairs demonstrated that the additional attenuation of photons by the standard table is 10.7% ± .8%. The average myocardial counts of prone imaging using the modified table was 218 ± 31, significantly higher than 194 ± 28 for the standard table ($p = 0.007$). It should be noted that this degree of attenuation is specific for the standard table used in this study, and that attenuation will vary depending on the thickness and composition of the imaging table. Figure 3 shows the short-axis images of the phantom from apex to base acquired through the modified table. Thallium-201 activity is essentially evenly distributed throughout the entire length of the "myocardium," and is free of artifactual defects. A mild "septal" increase or "hot spot" is also observed.

TABLE 3
Prone ^{201}Tl SPECT Overall Sensitivity and Specificity for Detection of Patients with Coronary Artery Disease and the Normalcy Rate in Patients with a Low Likelihood of Disease

	Sensitivity	Normalcy Rate	Specificity
Quantitative*	93% (28/30)	89% (49/55)	80% (4/5)
Visual	83% (25/30)	98% (54/55)	83% (5/6)

* p = ns for comparison to visual analysis.

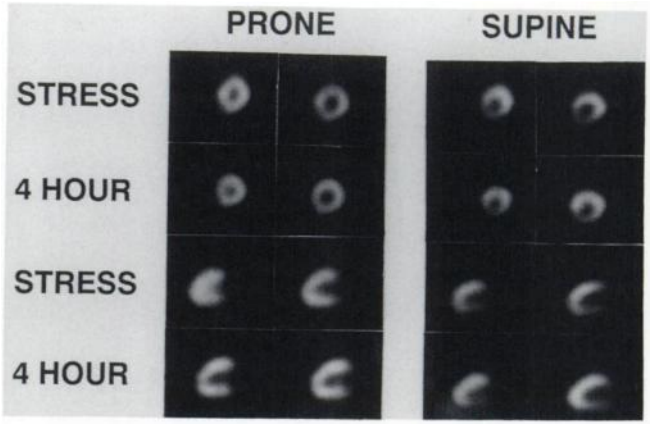

FIGURE 2. Prone (using the modified table) and supine ^{201}Tl SPECT of a normal patient. Representative stress and 4-hr redistribution short-axis views (top two rows) and vertical long-axis slices (bottom two rows) from different ventricular locations. With prone SPECT, the myocardial perfusion appeared to be normal, whereas the supine study shows a nonreversible inferior and inferoseptal defect.

Comparison Between Supine and Prone SPECT for Incidences of Patient Motion During SPECT Acquisitions

Comparisons of the demographics, clinical profile, exercise and ^{201}Tl data between the 100 patients who had ^{201}Tl studies using supine imaging and another 100 patients who had prone ^{201}Tl SPECT demonstrated a higher incidence of males (85% versus 62%, $p = 0.0002$) and a longer exercise duration (7.7 ± 2.9 versus 6.5 ± 3.0, $p = 0.008$) in the prone group (Table 1).

As shown in Table 6, when compared to supine imaging, the frequency of both severe and mild patient motion occurring during SPECT acquisitions were significantly lower with prone imaging.

DISCUSSION

Our study demonstrates that by using a specially designed table with a cutout under the cardiac area to minimize photon attenuation, and specific prone normal limits developed for this table, quantitative analysis of prone ^{201}Tl SPECT yielded high overall sensitivity and specificity for detection of coronary artery disease in the catheterized population, as well as high normalcy rates among patients with a low likelihood of coronary artery disease. The visual results were also similar to those described by Segall and Davis (*2*). Importantly, high specificity was shown by prone imaging for detection of disease in the right coronary artery. This finding is likely to be related to our observation that compared to supine imaging, prone SPECT provides significantly higher regional myocardial counts in the inferior wall and septum. Our findings also showed, however, that despite the use of a specially constructed table, the total myocardial counts with prone imaging are lower and the chest wall-to-detector distance is greater when compared to the supine position.

TABLE 4
Individual Vessel Sensitivity and Specificity for Prone ^{201}Tl SPECT

	Sensitivity				Specificity			
	Total	RCA	LAD	LCX	Total	RCA	LAD	LCX
Quantitative*	85% (45/53)	88% (15/17)	78% (14/18)	89% (16/18)	87% (45/52)	94% (17/18)	94% (16/17)	71% (12/17)
Visual	74% (39/53)	76% (13/17)	67% (12/18)	78% (12/18)	91% (50/55)	89% (17/19)	100% (18/18)	83% (15/18)

* p = ns for all comparisons to visual analysis.

Visual Versus Quantitative Approach

The results of quantitative prone SPECT were comparable to the results of visual analysis. This finding has also been reported for supine ^{201}Tl SPECT in a large patient population by DePasquale et al. (*17*). Quantitative approaches are still important in circumventing the problems of intra- and interobserver variability, which helps in the training of inexperienced readers and assists observers by providing an objective "second opinion." Additionally, quantitative ^{201}Tl SPECT has been previously shown to have a high degree of reproducibility (*18*), provides accurate assessment of myocardial perfusion defect size (*19, 20*) and shows a good correlation with the degree of coronary stenoses (*21,22*). Quantitative approaches may thus be clinically useful for the serial objective assessment of treatment efficacy.

Incidence and Degree of Severity of Patient Motion During SPECT Acquisition

Prone imaging appears to reduce the frequency and degree of patient motion, a potential cause of artifactual perfusion defects (*13,14*). With prone imaging, motion is probably reduced by having the anterior part of the chest, which contains the heart, immobilized against the table. Our results showed that severe motion occurred in 4% of supine ^{201}Tl SPECT studies, but in none by prone imaging. Furthermore, while a mild degree of patient motion was detected in 12% of the supine studies, it was noted in only 3.5% of the prone studies. In our experience, females with large breasts or patients with marked obesity generally prefer supine imaging.

Potential Pitfalls of Prone SPECT

In comparison to supine imaging, prone SPECT resulted in slightly lower total myocardial counts, most likely due to the observed increase in camera-to-chest wall distance.

TABLE 5
Prone ^{201}Tl SPECT Individual Vessel Sensitivity in Patients with no Prior Myocardial Infarction

	Total	RCA	LAD	LCX
Quantitative*	79% (26/33)	91% (10/11)	64% (7/11)	82% (9/11)
Visual	90% (23/33)	73% (8/11)	64% (7/11)	73% (8/11)

* p = ns for all comparisons to visual analysis.

Since increased camera to chest wall distance also reduces image resolution, this represents a major shortcoming of prone imaging. Figure 4 demonstrates a case example of prone imaging with a standard table in which the image quality is clearly inferior to that of the images acquired in the supine position. A narrow table (width: 11–13 in.) would be desirable to minimize camera-to-chest wall distance.

From our experience, a small, mild and nonreversible anterior/anteroseptal defect is occasionally observed with prone imaging, especially when the imaging is performed with a standard table (Fig. 5). This phenomenon is thought to represent attenuation by a rib or the sternum. As previously shown by Segall and Davis (*2*) with a cardiac magnetic resonance imaging case example in the prone position, the heart "flops" forward and comes to lie closer to the anterior chest wall. When closer to the heart, a bony structure such as a rib or the sternum would attenuate a greater proportion of the emitted photons. Our cardiac phantom prone SPECT demonstrated no artifactual defects (Fig. 3). This finding corroborates the hypothesis (but does not prove) that the small and discrete nonreversible anterior/anteroseptal wall defect observed in clinical prone SPECT may be caused by an anatomical structure between the heart and the camera. When imaging is performed on the modified table with a cut-out, the occasionally seen prone artifact is often small, easily recognized and usually does not pose a diagnostic dilemma, as reflected by the high normalcy rates and high LAD specificities for both

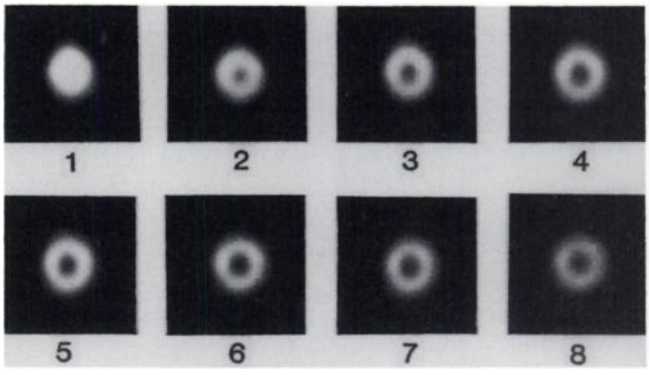

FIGURE 3. Prone SPECT images of a cardiac phantom from apex (segment 1) to base (segment 8) demonstrating even ^{201}Tl tracer distribution. Note the presence of small septal hot spot.

TABLE 6
Frequency of Patient Motion in Supine and Prone SPECT

	Prone	Supine	p
Number of patients	100	100	
Number of SPECT studies	200	200	
Motion			
Mild	3.5% (7/200)	12% (24/200)	<0.002
Severe	0	4% (8/200)	<0.005

visual and quantitative analyses in this study. The effect of combined breast tissue and prone imaging related attenuation in females is not known and would require further evaluation.

While a lateral hot spot is a known finding for supine ^{201}Tl SPECT, a small septal hot spot has been occasionally observed with prone imaging (Fig. 2). Due to the possible rotational and translational shift of the heart as a result of prone imaging, the left ventricular septum may lie closer to the detector compared to imaging in the supine position, resulting in the observed higher septal count density (Table 2). The visual perception of this phenomenon is exaggerated by the high regional contrast between the septum and the adjacent, more anteriorly placed anteroseptal/anterior wall, the latter being subject to the attenuating effect of the surrounding osseous structure as discussed above. In the phantom study, since such a attenuating structure was not present, the septal hot spot was not as readily discernible (Fig. 3). Although a hot spot is a potential cause of artifactual defects, in our experience it has not been noted to produce difficulty for visual interpretation.

Limitations

This study does not provide a direct comparison of diagnostic accuracy between prone and supine imaging in the same patient population. However, our prime objective was to derive and validate a new quantitative analysis for prone SPECT performed with a specially designed imaging table. Since we only developed normal limits for the male population, our results should not be used to predict diagnostic efficacy of prone SPECT for females. Although in our study it was shown that prone SPECT reduced the frequency and degree of patient motion, the issue of whether prone SPECT will result in a reduced incidence of motion-related artifactual perfusion defect has not been explored.

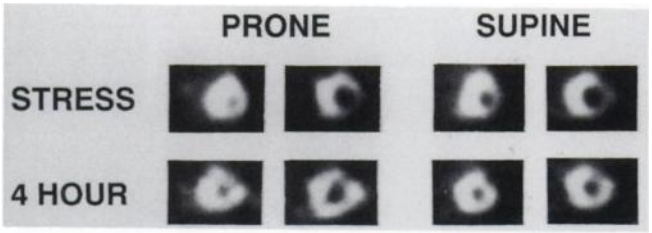

FIGURE 4. A case example illustrating inferior image quality of the representative prone ^{201}Tl SPECT short-axis tomograms, performed with a standard table (left) on an obese patient compared to supine SPECT (right). Note that the comparative worsening in image quality by prone imaging was more prominent on the 4-hr redistribution images due to fewer myocardial counts as compared to stress images.

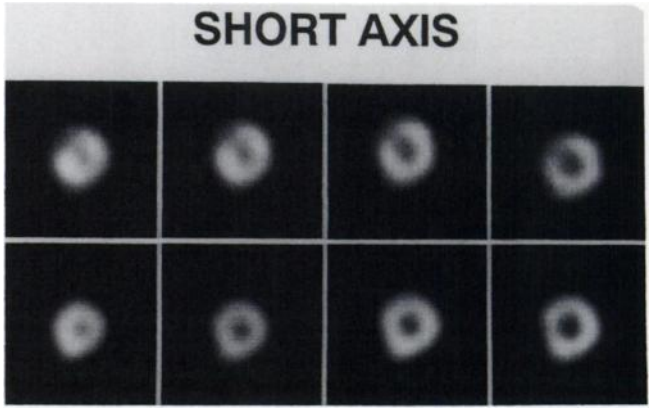

FIGURE 5. Representative stress ^{201}Tl short-axis slices (left to right = apex to base) of a patient with a low likelihood of coronary artery disease illustrating prone imaging artifact. The prone SPECT (top row) (using standard table with no cut-out center) had a small anteroseptal defect that was not present on supine imaging (bottom row).

CONCLUSION

When compared to supine imaging, ^{201}Tl prone SPECT produces higher counts in the inferior and septal regions of the left ventricle. In males, both visual and quantitative ^{201}Tl prone SPECT result in high overall specificity and accurate coronary artery disease localization, as well as high normalcy rates in patients with a low likelihood of disease. Because of the increased camera-to-chest wall distance and the resultant reduction in myocardial count rates and resolution compared to supine acquisition, as well as the occasionally seen artifactual anteroseptal/anterior wall defects, we recommend supine as the imaging position of choice for ^{201}Tl SPECT. Prone SPECT, however, provides an alternative imaging approach in patients who cannot tolerate supine acquisition or in whom inferior wall defects seen with supine imaging present a diagnostic dilemma. Prone imaging should also be considered when significant patient motion occurs during supine SPECT, necessitating repeat acquisition.

ACKNOWLEDGMENTS

We are grateful to Mark Hyun, CNMT, Jim Bietendorf, CNMT, and Ken Nichols PhD for expert technical assistance, and to Mitzi Escuin for professional secretarial assistance. This study was supported in part by SCOR grant 7651 from the National Institutes of Health, Specialized Center of Research, Bethesda, MD and a grant from the American Heart Association. Greater Los Angeles Affiliate, Los Angeles, CA. This work was presented in part at the 37th Annual Scientific Session of the Society of Nuclear Medicine, Washington DC, June, 1990.

REFERENCES

1. Esquerre J-P, Coca FJ, Martinez SJ, Guiraud RF. Prone decubitus: a solution to inferior wall attenuation in thallium-201 myocardial tomography. *J Nucl Med* 1989;30:398–401.
2. Segall GM, Davis MJ. Prone versus supine thallium myocardial SPECT: a method to decrease artifactual inferior defects. *J Nucl Med* 1989;30: 548–555.
3. Diamond GA, Forrester JS. Analysis of probability as an aid in the clinical diagnosis of coronary artery disease. *N Engl J Med* 1979;300:1350–1358.
4. Diamond GA, Forrester JS, Hirsch M, et al. Application of conditional probability analysis to the clinical diagnosis of coronary artery disease. *J Clin Invest* 1980;65:1210–1221.
5. Rozanski A, Diamond GA, Forrester JS, et al. Alternative referent standards for cardiac normality. Implications for diagnostic testing. *Ann Intern Med* 1984;101:164–171.
6. Maddahi J, Van Train K, Prigent F, et al. Quantitative single photon emission computerized thallium-201 tomography for evaluation of coronary artery disease: optimization and prospective validation of a new technique. *J Am Coll Cardiol* 1989;14:1689–1699.
7. Van Train K, Maddahi J, Berman DS, et al. Quantitative analysis of tomographic stress thallium-201 myocardial scintigrams: A multicenter trial. *J Nucl Med* 1990;31:1168–1179.
8. Chouraqui P, Maddahi J, Ostrzega E, et al. Quantitative exercise thallium-201 rotational tomography for evaluation of patients with prior myocardial infarction. *Am J Cardiol* 1990;66:151–157.
9. Kiat H, Berman DS, Maddahi J, et al. Late reversibility of tomographic myocardial thallium-201 defects: an accurate myocardial viability. *J Am Coll Cardiol* 1988;12:955–963.
10. Yang LD, Berman DS, Kiat H, et al. The frequency of late reversibility in SPECT thallium-201 stress redistribution studies. *J Am Coll Cardiol* 1990; 15:334–340.
11. Prigent F, Maddahi J, Garcia E, et al. Non-invasive quantification of the extent of jeopardized myocardium in patients with single-vessel disease by stress thallium-201 single photon emission computerized rotational tomography. *Am Heart J* 1986;111:578–586.
12. Kiat H, Maddahi J, Roy L, Friedman JD, Berman DS. Comparison of Tc-99m methoxy isobutyl isonitrile with Tl-201 imaging by planar and SPECT technique for assessment of coronary artery disease. *Am Heart J* 1989; 117:1–11.
13. Friedman J, Van Train K, Maddahi J, et al. "Upward creep" of the heart. A frequent source of false-positive reversible defects on Tl-201 stress-redistribution SPECT. *J Nucl Med* 1989;30:1718–1722.
14. Friedman J, Berman DS, Van Train K, et al. Patient motion in thallium-201 myocardial SPECT imaging: An easily identified frequent source of artifactual defect. *Clin Nucl Med* 1988;135:321–324.
15. SAS Institute INC. SAS user's guide: Statistics. Version 5 edition. Cary, NC, 1985.
16. Dixon WJ, ed. *BMDP statistical software*—1985 printing. Berkrley: University of California Press; 1985.
17. DePasquale EE, Nody AC, DePuey EG, et al. Quantitative rotational thallium-201 tomography for identifying and localizing coronary artery disease. *Circulation* 1988;77:316–327.
18. Prigent F, Berman D, Bellil D, et al. Reproducibility of quantitative indices of follow-up SPECT one year in stable diagnostic patients [Abstract]. *J Nucl Med* 1989;30:729.
19. Prigent F, Maddahi J, Garcia EV, Satoh Y, Van Train K, Berman DS. Quantification of myocardial infarct size by thallium-201 single photon emission computerized tomography: experimental validation in the dog. *Circulation* 1986;74:852–861.
20. Prigent F, Maddahi J, Garcia EV, Resser K, Lew AS, Berman DS. Comparative methods for quantifying myocardial infarct size by thallium-201 SPECT. *J Nucl Med* 1987;28:325–333.
21. Papanicolaou M, Van Train KF, Kiat H, Eigler N, Friedman J, Berman D. Quantitative severity of myocardial stress thallium-201 SPECT defects in relation to quantitative coronary angiography. *Circulation* 1990;82: III–321.
22. Hadjimiltiades S, Watson R, Hakki A-H, Heo J, Iskandrian AS. Relation between myocardial thallium-201 kinetics during exercise and quantitative coronary angiography in patients with one vessel coronary artery disease. *J Am Coll Cardiol* 1989;13:1301–1308.